

Statistical exploration approach to design centring

R.S. Soin, B.Sc(Eng.), A.C.G.I., Ph.D., and
R. Spence, B.Sc.(Eng.), Ph.D., D.I.C., C.Eng., F.I.E.E., Fel.I.E.E.E.

Indexing terms: Circuit theory and design, Computer applications, Mathematical techniques

Abstract: This paper addresses the problem of design centering; that is, the maximisation of manufacturing yield by suitable choice of nominal component parameter values while the tolerances and form of the probability density function of the parameters are assumed fixed. In the technique discussed, Monte Carlo analysis is performed for a particular set of nominal values. The results of the analysis are then used both to estimate yield and to choose new nominal values which are expected to increase yield. The procedure is repeated until no further increases in yield occur. The heuristic algorithm employed is based on the relative positions, in component space, of the centres of gravity of the pass and fail circuits as identified by the Monte Carlo analysis. The effectiveness of the procedure is illustrated for a number of circuit examples ranging from seven to forty-three toleranced components. Experience strongly suggests that the number of iterations required is independent of dimensionality (the number of toleranced components). Unlike other methods of design centering, the method does not require assumptions regarding the convexity or connectivity of the region of acceptability. Finally, to moderate the computational cost of iteratively performing Monte Carlo analysis, special sampling schemes are employed which reduce the number of sample circuits required to be analysed by each Monte Carlo analysis.

1 Introduction

In the design of a mass-produced circuit it must constantly be borne in mind that the component parameter values are subject to statistical spreads due to uncertainties in the component manufacturing process. As a consequence, the properties of the manufactured circuit will exhibit statistical variation from one sample to another. Indeed, the extent of this variation may be such that some of the manufactured circuits fail to meet the specifications placed on their properties by the customer. That fraction of the manufactured circuits which meets the specifications is referred to as the manufacturing yield.

It is clearly useful to be able to maximise the yield, and the principal method for doing this is called 'design centering'. In this approach, component tolerances are left unchanged but their nominal values are chosen more appropriately. After so doing, it may be possible further to reduce the unit cost of the manufactured circuit by the assignment of new component tolerances: whether the tolerances are increased or decreased will depend upon the cost/tolerance relationship of each component.

Since design centering will normally precede tolerance assignment, or may in any case be the only realistic means of enhancing the yield and reducing cost (e.g. integrated circuits, mechanical filters), it is an important technique in its own right and is the subject of this paper.

Several deterministic methods of design centering have been proposed.^{1,2} These, however, require the identification of combinations of component values such that the circuit just fails to meet the performance requirements, a characteristic responsible for the computational cost becoming prohibitive if the number of toleranced components exceeds about five. Additionally, deterministic methods suffer from limitations upon the nature of the performance specifications. By contrast, the method proposed in this paper employs the statistical exploration approach and, as a consequence, does not suffer from the same limitations. Moreover, it is equally valid for nonlinear

as well as linear circuits, and is easy to implement in software.

In the approach to design centering described in this paper, the yield is first estimated by a conventional Monte Carlo analysis. This analysis constitutes a statistical exploration of a region defined by component nominal values and tolerances, within the multiparameter component space whose axes correspond to the toleranced parameters. However, this calculation is used not only to estimate the manufacturing yield: the spatial information it generates is also used to decide on a new location, in multiparameter component space, for the nominal component values. The process is then repeated until no further increase in yield is sought.

2 Design centering

Consider a circuit whose behaviour is determined by K toleranced component parameters. The parameters may be associated on a one-to-one basis with individual components (e.g. R, L, C) or may constitute part of a parametric model of a device such as a transistor or an operational amplifier. We denote by the vector P the values of these K parameters, viz:

$$P = p_1 p_2, \dots, p_K$$

and we employ a superscript 'o' to denote the vector of nominal parameter values:

$$P^o = p_1^o p_2^o \dots p_K^o$$

The tolerance vector $T = t_1 t_2, \dots, t_k$ defines the tolerances on the parameters, such that

$$(p_j^o - t_j) \leq p_j \leq (p_j^o + t_j) \quad j = 1, \dots, K \quad (1)$$

Consider also that the circuit is subject to m performance requirements of the form

$$\underline{f}_i < f_i(P) < \bar{f}_i \quad i = 1, \dots, m \quad (2)$$

The constants \bar{f}_i and \underline{f}_i are, respectively, the upper and lower allowable limits on the i th performance function of the circuit. The performance function $f_i(P)$ may be any

Paper 1052G, first received 22nd August 1980

Dr. Soin is with Philips Research Laboratories, Redhill, Surrey, England and Dr. Spence is with the Department of Electrical Engineering, Imperial College of Science and Technology, Exhibition Road, London SW7 2BT, England

quiescent-, frequency- or time-domain property of the circuit.

Simultaneous consideration of the tolerated components, the circuit's performance and the specifications is aided by reference to a multiparameter component space, each of whose axes is associated with a tolerated component. The tolerances on the parameters define a tolerance region R_T which, for the simple but illustrative case of two uncorrelated components, is a rectangle (Fig. 1). Thus, a vector P satisfying exprs. 1, i.e. a manufactured circuit, is represented by a point within R_T . In the same multiparameter component space, the region of acceptability R_A contains those parameter values which, together, describe a circuit which satisfies the specifications (expr. 2). As illustrated in Fig. 1, the boundary of R_A is typically composed of a number of segments, each associated with a different performance specification. In most cases, the boundary will be irregular, may contain both concave and convex segments, and is unsuited to analytic description.

If the region R_T does not lie wholly within the region of acceptability R_A , as is the case in the illustration, then it is likely that some of the manufactured circuits will not meet the specifications. These unacceptable circuits are represented by the hatched areas in Fig. 1.

The yield Y is the expectation that a manufactured circuit will meet the specifications. In the illustration of Fig. 1, if all values of a component p_j between its limits $(p_j^o - t_j)$ and $(p_j^o + t_j)$ are equally probable, and if there is no correlation between component values, then the yield Y is the area of R_T lying within R_A (i.e. $R_T \cap R_A$), expressed as a fraction of the area of R_T . For more than two tolerated components, the areas become hypervolumes. In the case where the distribution of component values is not uniform and/or when component values are correlated, every point in R_T may be considered to have a weight proportional to the value of the component probability density function at that point. The yield may then be taken to be the ratio of the weighted volume of $(R_T \cap R_A)$

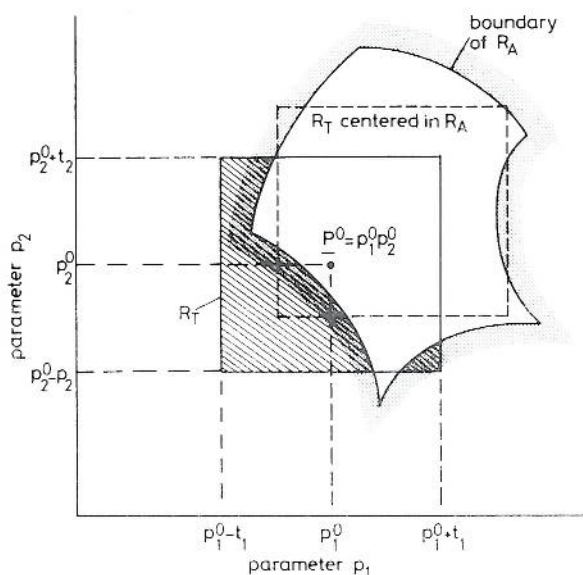


Fig. 1 Tolerance region R_T and region of acceptability R_A in multiparameter component space

Hatched area is associated with circuits that fail the specification. The result of centering R_T within R_A is shown as broken lines

to that of R_T . Yield is defined more rigorously as a multi-dimensional integral in Appendix 10.1.

The problem addressed in this paper is that of maximising yield through variation of the nominal parameter values P^o , while keeping tolerances T constant:

$$\text{Maximise } Y(P^o, T) \quad \text{by choice of } P^o \quad (3)$$

Such a maximisation can be interpreted geometrically as the maximisation of the intersection $R_T \cap R_A$ by centering R_T within R_A (Fig. 1). Most of our attention will be directed to satisfying expr. 3 for those situations in which components are uniformly distributed and uncorrelated. As explained later, other cases will often be handled simply and adequately in the very last iteration of the algorithm to be described. The changes in nominal values typically encountered in design-centering procedures are rarely of a magnitude such that permissible limits to nominal values (also called box constraints³) are violated. Therefore, expr. 3 can safely be treated as an unconstrained optimisation problem.

3 Centres of gravity algorithm

Viewed very simply, a design-centering procedure can be considered to comprise two tasks:

- (a) estimation of yield Y
- (b) choice of the new nominal point P^o .

Although (a) will later be extended to include an estimate of the sign of any change in Y consequent on a new choice of P^o , we shall first consider the straightforward estimation of yield and the choice of a new P^o .

For an increasing number of tolerated components, and hence an increasing dimensionality of component space, it is impracticable to estimate yield by means of a deterministic numerical integration method. We therefore employ, instead, a conventional Monte Carlo analysis which constitutes a random sampling – or ‘statistical exploration’ – of the tolerance region R_T . Now, Monte Carlo analysis is conventionally regarded as an expensive computational procedure, whose cost is proportional to the number of random sample circuits analysed. It has, however, the paramount advantage that the number of random circuit samples required to be analysed for a specific confidence in the yield estimate is independent of the number of component parameters describing the circuit. It is this single property that allows the statistical exploration approach to design centering to be applied successfully to circuits containing up to 43 tolerated components. Moreover, as will be shown later, methods have been devised for effecting a considerable reduction in the number of Monte Carlo samples required.

The basis for the choice of the new nominal point P^o is easily described. Following the Monte Carlo analysis, which identifies each circuit sample as ‘pass’ or ‘fail’ accordingly, the centres of gravity of both the pass and fail samples in component space are determined. The line joining these two points (Fig. 2) is then parallel to the direction in which P^o is to be moved, with the movement occurring in the direction G_F to G_P , respectively the centres of gravity of the fail and pass samples. The actual distance moved by P^o is some fraction λ of the distance between the two centres of gravity.

After so moving the nominal point, the process (estimation of Y followed by choice of P^o) is repeated until either 100% yield is obtained or a further increase in yield

appears unlikely. Thus, the structure of the design centering scheme is as shown in Fig. 3. We now discuss the calculation of the direction of movement of P^0 and the choice step size λ .

3.1 Direction of movement of P^0

Let G_P , the centre of gravity of the pass circuits, be defined by the corresponding values of the component parameters:

$$G_P = g_{P_1} g_{P_2}, \dots, g_{P_K}$$

An estimate of G_P can then be made as follows. Let N_P and N_F be the number of pass and fail circuits respectively. Also let p_{ij} denote the value of the i th component parameter of the j th sample circuit. Then

$$g_{P_i} = \frac{1}{N_P} \sum_{\substack{\text{pass} \\ \text{circuits}}} p_{ij}, \quad i = 1, \dots, K \quad (4)$$

Similarly for the fail centre of gravity

$$G_F = g_{F_1} g_{F_2} \dots g_{F_K}$$

and

$$g_{F_i} = \frac{1}{N_F} \sum_{\substack{\text{fail} \\ \text{circuits}}} p_{ij}, \quad i = 1, \dots, K \quad (5)$$

If we denote two successive iterations (i.e. two successive Monte Carlo analyses) by subscripts M and $M+1$, the

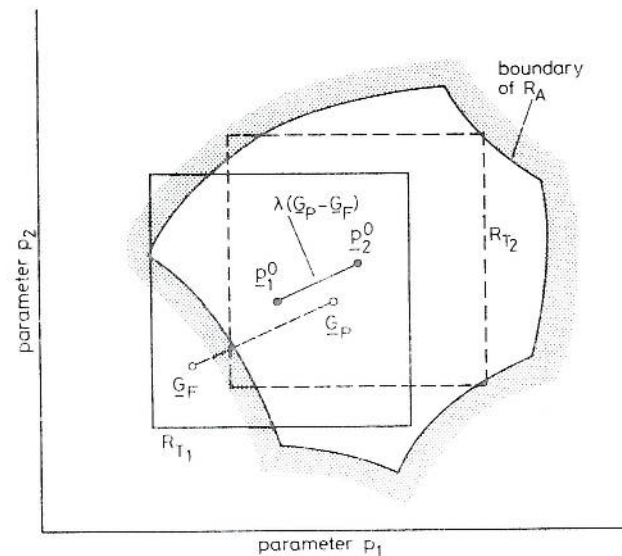


Fig. 2 Relation of movement of nominal point to centres of gravity of pass and fail circuits

proposed relationship between the old and new design centres is:

$$P_{M+1}^0 = P_M^0 + \lambda(G_{PM} - G_{FM}) \quad (6)$$

For later reference we denote by ΔG_M the separation $G_{PM} - G_{FM}$ between the centres of gravity (as shown in Fig. 2) and by $\Delta g_1, \Delta g_2, \dots, \Delta g_K$ the co-ordinates of ΔG_M .

3.2 Choice of step size

In view of the cost of obtaining a yield estimate by Monte Carlo analysis, it is inadvisable to perform a unidirectional search parallel to ΔG_M and passing through P_M^0 to find a yield maximum. Rather, a single value of λ must be chosen at each iteration and only discarded if no improvement in yield appears to be obtained (i.e. if $Y_{M+1} \leq Y_M$). Initial experience suggested values of λ between 0.5 and 1.0.⁴ Later, a rule (to be described below) was formulated which usually leads to substantial increases in yield, and rarely to a decrease.

The rule for the choice of λ is derived with reference to Fig. 4 which depicts the tolerance regions of two successive iterations: for simplicity, and without loss of generality, a 2-dimensional example is shown. Based on the designation of the parts of the tolerance regions shown in Fig. 4, the yields of the two iterations can be expressed as

$$Y_{M+1} = V_{(B \cup C) \cap R_A} \quad (7)$$

$$Y_M = V_{(A \cup B) \cap R_A} \quad (8)$$

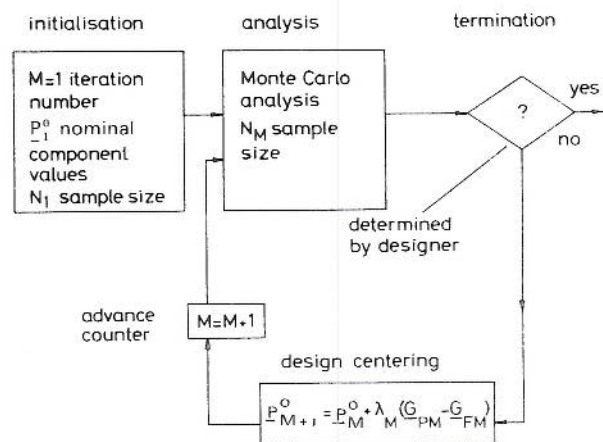


Fig. 3 Flow chart for centres-of-gravity method of design centering

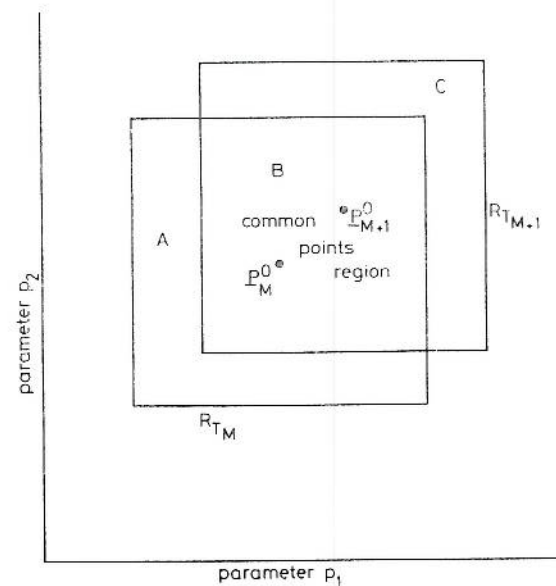


Fig. 4 Common points region (B) containing sample points from R_{T_M} that can be reused for $R_{T_{M+1}}$

$$A \triangleq R_{T_M} \cap \bar{R}_{T_{M+1}}, B \triangleq R_{T_M} \cap R_{T_{M+1}}, C \triangleq \bar{R}_{T_M} \cap R_{T_{M+1}}$$

where V denotes the volume of the region normalised with respect to the volume ($V_A + V_B$) of the tolerance region. Also we denote by

$$\Delta Y_M = Y_{M+1} - Y_M \quad (9)$$

the difference of the two yields.

We consider now a limit case in which two conditions hold:

- (a) 100% yield can be achieved with the given tolerances
- (b) it can be achieved by one step in the iteration.

Condition (a) implies that

$$\Delta Y_M = 1 - Y_M \quad (10)$$

while, for condition (b) to be satisfied

$$V_C = 1 - Y_M \quad (11)$$

The volume V_C can be expressed in terms of the tolerances t_i , the direction ΔG_M and step size λ as:

$$\prod_{i=1}^K 2t_i - \prod_{i=1}^K (2t_i - \lambda \Delta g_i) = 1 - Y_M \quad (12)$$

In practice, the maximum obtainable yield is often less than 100% and also cannot be achieved in one iteration. In this case, the equality (eqn. 12) must be replaced by an inequality to obtain a rule for choosing λ :

$$\prod_{i=1}^K 2t_i - \prod_{i=1}^K (2t_i - \lambda \Delta g_i) \leq 1 - Y_M \quad (13)$$

Since little is known about the shape of typical regions of acceptability, a more precise rule for choosing λ is difficult to obtain. In view of this uncertainty, and because expr. 13 cannot be rearranged to give λ explicitly, we compute V_C for several values of λ (typically between 0.1 and 1.5 in steps of 0.1). A value of λ which satisfies expr. 13 is then chosen, although the designer must be prepared to take corrective action (i.e. a reduced value of λ), should the yield appear to decrease. However, experience has shown that, as the designer gains familiarity with the algorithm, he can exercise effective judgment in the choice of step length.

4 Confidence of correct yield ranking

In the basic form of the algorithm described above, the yield Y is estimated at each new location of the nominal point P^o as it is determined by the relation of eqn. 6. However, uncertainty is always associated with the estimate of yield. For a reasonably large sample size N , the sampling distribution of the yield estimate provided by Monte Carlo analysis is approximately normal with a mean of Y (the true value of the yield) and a standard deviation $\sigma = \sqrt{Y(1-Y)/N}$. The value of Y is not known, of course; hence, to be able to compute confidence intervals associated with specific yield estimates, we estimate the standard deviations as $\sigma_{\hat{Y}} = \sqrt{\hat{Y}(1-\hat{Y})/N}$, where \hat{Y} is an estimate* of the unknown yield Y . Then we may say, for example, that the 95% confidence interval for yield is $\hat{Y} \pm 2\sigma_{\hat{Y}}$. For this reason, an apparent increase in yield may occur during an iteration wherein the actual yield suffers a decrease. It is therefore necessary to pay attention, not only to the estimated yield (the quantity of paramount interest), but

also to whether a particular iteration has been worthwhile in the sense of achieving an increase in yield.

The distribution of $\Delta \hat{Y}_M$ (the estimated change in yield) is the difference between two normally distributed random variables and is also normal. The variance of $\Delta \hat{Y}_M$ will be given by

$$\begin{aligned} \text{Var}(\Delta \hat{Y}_M) &= \text{Var}(\hat{Y}_M) + \text{Var}(\hat{Y}_{M+1}) - \\ &2 \text{Cov}(\hat{Y}_M, \hat{Y}_{M+1}) \end{aligned} \quad (14)$$

For illustration, we shall consider ΔY_M to be positive, and the sampling distribution of ΔY_M is shown in Fig. 5.

Since we do not know the true value of ΔY_M , we take $\Delta \hat{Y}_M$ to be the centre of this distribution, and estimate the variance according to eqn. 14. In this way, we obtain the confidence of correct ranking. The confidence in the assertion that ΔY_M is positive is then the (shaded) area under the curve to the right of the abscissa. Formally, the area is equal to $\frac{1}{2} + \text{erf}(\Delta Y_M / \sigma_{\Delta Y_M})$, where $\sigma_{\Delta Y_M}$ is the standard deviation of ΔY_M , i.e. $\sigma_{\Delta Y} = \sqrt{\text{Var}(\Delta Y_M)}$, and $\text{erf}(\cdot)$ is the error function defined as

$$\text{erf}(t) = \frac{1}{\sqrt{2\pi}} \int_0^t \exp(-x^2/2) dx$$

The error function is a monotonically increasing function.

5 Sampling schemes for reducing computational cost

If straightforward and independent Monte Carlo analyses are performed at two successive iterations, the covariance term in eqn. 14 is zero, and quite a large number of samples

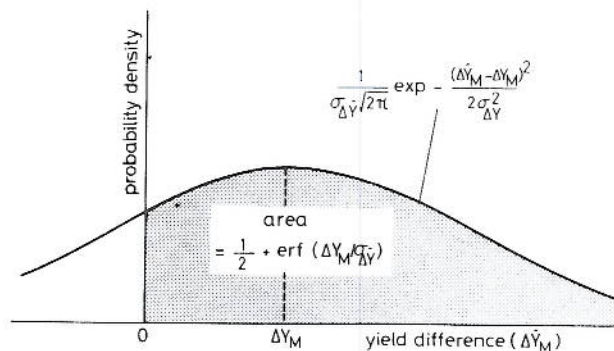


Fig. 5 Sampling distribution of difference ($\Delta \hat{Y}_M$) in yield estimates between two successive iterations

at each iteration might be necessary to obtain a reasonable confidence of correct ranking. It is therefore important to seek sampling schemes that will achieve a high confidence level at an acceptably low computational cost. We now examine two such schemes: briefly, with reference to Fig. 5, the 'correlated sampling scheme' squeezes the distribution inwards towards the mean (Fig. 6), while the principal objective of the 'common points scheme' is to shift the mean to the right (Fig. 6). With reference to the above definition of the error function, since the confidence of correct ranking increases with increasing value of the argument of the error function, the two schemes attempt to increase this argument by either decreasing $\sigma_{\Delta Y}$ (correlated sampling) or by increasing ΔY (common points). The ideas behind the two sampling schemes are discussed below while, in Appendixes 10.2 and 10.3, we list particular

*Henceforth, superscript hat denotes estimate of relevant quantity

algorithms incorporating either scheme into the overall design-centering strategy.

5.1 Correlated sampling

The object of correlated sampling is to introduce a positive covariance (see eqn. 14) between the yield estimates at the M th and $M+1$ th iterations, thereby reducing $\sigma_{\Delta Y}^2$, for a given sample size, below what would apply to independent Monte Carlo analyses. It is effected by using the same random numbers for obtaining component values for the sample circuits of successive Monte Carlo analyses. In other words, the samples at each iteration have the same location relative to one another: they are merely shifted, together, in the same manner that P^o is shifted.

Broadly speaking, the precision of the estimate of yield difference is enhanced because the dependence between the two individual yield estimates is such that, when one result is overestimated (or underestimated) by sampling variations, then so is the other one, by roughly the same amount. A detailed comparison of independent and correlated sampling has been made by Becker.⁵ Although the correlated sampling scheme has the advantage that it may be used for any form of component probability density function (e.g. uniform, bimodal, normal), the scheme to be described next, although essentially restricted to uniform parameter distributions, is more efficient: in other words, for a given confidence of correct ranking, the common points scheme requires a smaller number of circuit analyses.

5.2 Common points scheme

The essence of the common points scheme is that, if the circuit has already been analysed at a sample point which also happens to be contained within the new tolerance region, then use should be made of the information provided by that analysis. Again, with reference to the 2-dimensional example (Fig. 4), using the same notation as before and setting $M=1$, it is clear that the samples associated with R_{T_1} in iteration 1, but falling within region B which is common to R_{T_2} , can be employed, together with new samples taken in region C , to estimate the yield associated with tolerance region R_{T_2} . Volume B is referred to as the common region, and the sample points within it as the common points.

To appreciate the advantage of the common points scheme, it is convenient first to consider the concept of 'partial yield'. For example, of the N samples generated within R_{T_1} , assume that N_A fall within region A and N_B within region B ($N=N_A+N_B$). If the number of passes within region A is N_{AP} , we can estimate the partial yield of region A as $\hat{Y}_A=N_{AP}/N_A$. Similarly, the partial yield Y_B of region B can be estimated. The partial yields can then be used to obtain an estimate of the yield associated with region R_{T_1} according to

$$\hat{Y}_1 = V_A \hat{Y}_A + V_B \hat{Y}_B \quad (15)$$

since all volumes are normalised with respect to the volume of the tolerance regions.

Within the new tolerance region R_{T_2} , samples need only be generated within region C : these will be distributed uniformly and for convenience will normally be N_C in number, so that both R_{T_1} and R_{T_2} contain an identical number of samples. If the partial yield of region C is

estimated as \hat{Y}_C , the yield associated with R_{T_2} can then be estimated as

$$\hat{Y}_2 = V_B \hat{Y}_B + V_C \hat{Y}_C \quad (16)$$

By reference to eqns. 15 and 16, the estimated difference in yield between tolerance regions 1 and 2 can be written as

$$\Delta \hat{Y} = V_C \hat{Y}_C - V_A \hat{Y}_A \quad (17)$$

or

$$\Delta \hat{Y} = V_C (\hat{Y}_C - \hat{Y}_A) \quad (18)$$

Because the confidence of correctly ranking Y_1 and Y_2 is identical with that of ranking the partial yields Y_A and Y_C , it is convenient now to turn our attention to the difference in partial yields ($Y_C - Y_A$) denoted by ΔPY . Since the sampling distributions of the partial yield estimates \hat{Y}_C and \hat{Y}_A are normal, so will be that of their difference $\Delta \hat{PY}$, as is illustrated in Fig. 6. An estimate of ΔPY is then provided by

$$\Delta \hat{PY} = \hat{Y}_C - \hat{Y}_A \quad (19)$$

However, from eqn. 17, we deduce that

$$\Delta \hat{Y} = V_C \cdot \Delta \hat{PY} \quad (20)$$

Recalling that V_C is the volume of region C normalised with respect to the volume of the tolerance region, it is seen that the true (or estimated) partial yield difference ΔPY will be greater than (and in practice usually much greater than) the true or estimated yield difference as is illustrated in Fig. 6. Since the sample points in A and C are uncor-

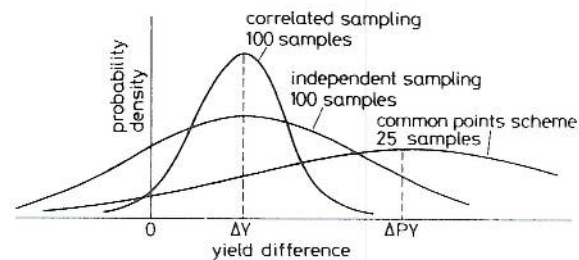


Fig. 6 Illustrating differences between sampling distribution of yield difference estimator for independent sampling, correlated sampling and common points scheme

related, the variance $\sigma_{\Delta PY}^2$ of the difference of the partial yields can be expressed as

$$\sigma_{\Delta PY}^2 = \sigma_{\hat{Y}_A}^2 + \sigma_{\hat{Y}_C}^2 \quad (21)$$

by reference to eqn. 14. The individual variances appearing in eqn. 21 can be estimated from

$$\hat{\sigma}_{\hat{Y}_A}^2 = \frac{\hat{Y}_A(1-\hat{Y}_A)}{N_A} \quad \text{and} \quad \hat{\sigma}_{\hat{Y}_C}^2 = \frac{\hat{Y}_C(1-\hat{Y}_C)}{N_C}$$

Normally, in view of the smaller number of samples selected in regions A and C when compared with B , the variance $\sigma_{\Delta PY}^2$ will be larger than that ($\sigma_{\Delta Y}^2$) associated with uncorrelated sampling, as reflected in Fig. 6.

The confidence of correctly ranking the partial yield estimates, and hence the overall yield estimates, is now given by:

$$\frac{1}{2} + \text{erf}(\Delta \hat{PY} / \hat{\sigma}_{\Delta PY}) \quad (22)$$

Compared with uncorrelated sampling, we have increased both the factor ΔY (by considering partial yields) and the standard deviation $\sigma_{\Delta Y}$ (there are fewer samples), but the overall effect is to increase the ratio. It is unfortunate that no simple relation connecting the standard deviations $\sigma_{\Delta Y}$ and $\sigma_{\Delta P Y}$ can be obtained, but it has been found in practice that the ratio, and hence the confidence of correct ranking, is enhanced in the common points scheme. It should also be borne in mind that, even in the limit where $\Delta P Y / \sigma_{\Delta P Y}$ is unchanged, the use of the common points scheme leads to a considerable saving in computational effort.

6 Circuit examples and results

The effectiveness of the design-centering strategy is demonstrated by application to three circuit examples, as follows:

6.1 Highpass filter circuit⁶

The circuit diagram, a typical shape of response and the performance constraints are illustrated in Figs. 7a and b. Fig. 8 summarises the results of applying the design-centering algorithm when tolerances at 5% and uniform p.d.f.s

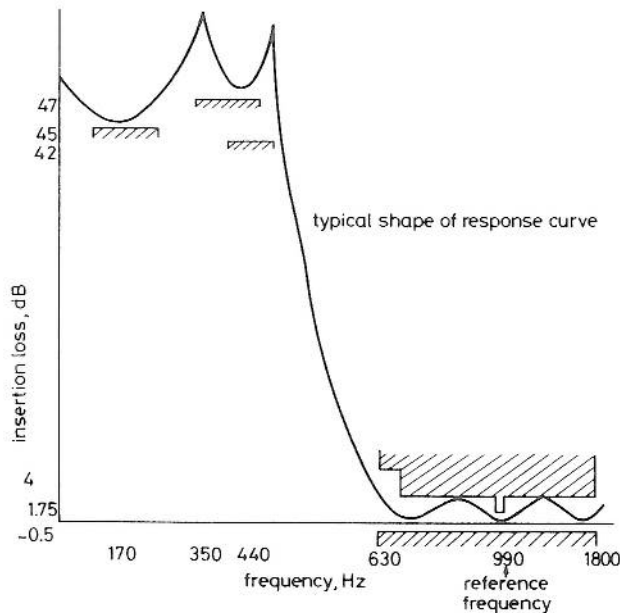
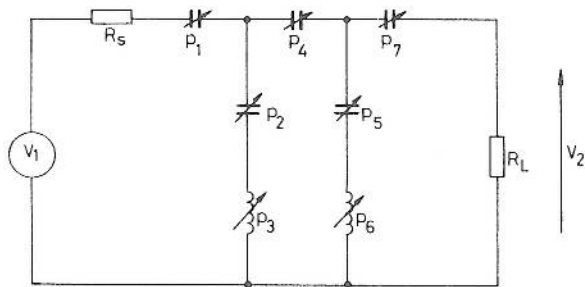


Fig. 7 Passive highpass filter

a Circuit diagram
Arrows indicate toleranced components
Insertion loss is $20 \log |V_2(j\omega)/V_1(j\omega)|$

b Performance requirements
Frequencies tested: 170, 350, 440, 630, 650, 720, 740, 760, 940, 1040, 1800 Hz

were assumed for all components subject to tolerance. The 95% confidence interval associated with each yield estimate is indicated, as is the value of step size λ chosen after each iteration. The common points scheme was used, and the total number of circuit analyses performed for each iteration is indicated, together with the confidence of correctly ranking iterates as described in Section 5. The available sample size was chosen to be 100; hence, for example, at iteration number two, 71 analyses from the previous iteration were reused and, for iteration three, 77 were reused. Monte Carlo analyses employing 500 samples each were performed using the same design centres as for the first and last iterations and confirmed the yield increases suggested by the design-centering strategy.

For the same circuit, Fig. 9 relates to the situation where

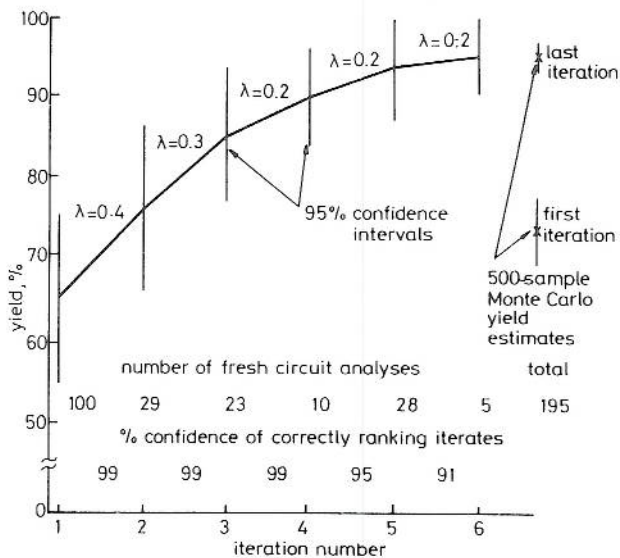


Fig. 8 Yield trajectory for highpass filter assuming 5% tolerances and uniform distributions

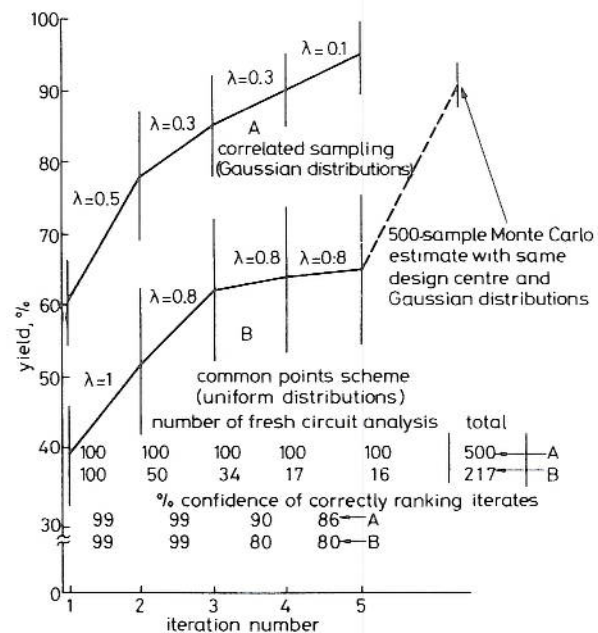


Fig. 9 Yield trajectories for highpass filter, assuming 10% tolerances and both Gaussian (A) and uniform (B) distributions

the component parameter $pdf \phi(P, P^0, T)$ is truncated K -variate Gaussian, i.e.

$$\phi(P, P^0, T) = \prod_{i=1}^K \frac{1}{\sigma_i \sqrt{2\pi}} \exp \left\{ -\frac{(p_i - p_i^0)^2}{2\sigma_i^2} \right\} \quad (23)$$

for $(p_i^0 - t_i) \leq p_i \leq (p_i^0 + t_i)$
 $= 0$ otherwise

and $\sigma_i = t_i/3$, say

Whereas such a situation may easily be handled by the scheme employing correlated sampling, the common points scheme is not directly applicable. However, in order to exploit the computational efficiency of the latter scheme, it was suggested that a satisfactory approach might be to assume a uniform p.d.f., to employ the common points scheme until further yield increases appear unlikely, and then to switch over to correlated sampling, and the correct p.d.f., as in eqn. 23. In other words it was postulated that there would be insufficient difference between the design centres associated with the two distributions to warrant discarding completely the computational advantage of the common points scheme. The upper curve of Fig. 9 illustrates the straightforward application of the correlated sampling scheme using the p.d.f. of eqn. 23, where all the components have fixed tolerances which are 10% of their initial nominal values. The final yield estimate was 94% after five iterations using a total of 500 circuit analyses. The lower curve refers to the common points scheme, assuming a uniform p.d.f. with the same tolerances, but with a change to a single 500 sample yield estimate (of 90%) using the p.d.f. of eqn. 23, following the fifth iteration. The proximity of the final yield estimates (94% and 90%) suggests that the proposed scheme for handling nonuniform distributions may well be an effective one.

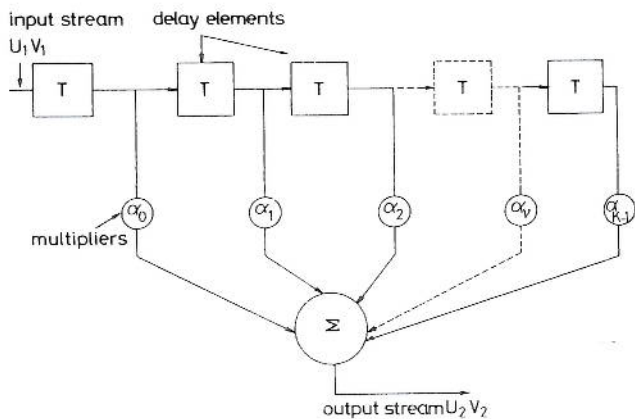


Fig. 10 General structure of transversal filter

6.2 Transversal filter circuit⁷

In support of the assertion that the proposed strategy is effective independently of the dimensionality of the circuit, we now discuss a circuit comprising 43 toleranced components. The circuit belongs to a family of transversal filters⁷ to be manufactured using charge-coupled devices. The basic structure of a transversal filter is shown in Fig. 10. The circuit operates on sampled values of an analogue signal. The input signal is passed through a cascade of delay elements. The output of each delay element is multiplied

by a particular coefficient and the multiplied outputs are summed to form the overall output of the filter. The response of the circuit for both frequency and time domains can be summarised as:

Time domain:

$$U_2(t) = \sum_{\nu=0}^{K-1} \alpha_{\nu} U_1(t - \nu T_s)$$

Frequency domain:

$$V_2(j\omega) = \sum_{\nu=0}^{K-1} \alpha_{\nu} V_1(j\omega) e^{-j\omega T_s}$$

where T_s , the intersample time interval, is related to the sampling frequency f_s as $T_s = 1/f_s$.

The filter coefficients $\alpha_i (i = 0, \dots, K-1)$ are defined by a capacitance which is proportional to the area of an electrode in an integrated circuit.⁷ Owing to the uncertainties of the manufacturing process, the values of these coefficients are subject to statistical variation.

Design centering was performed on a transversal filter with 43 variable coefficients. The applicable frequency-domain specifications are shown in Fig. 11. The nominal values of the coefficients were in the range -1 to 1 and the largest value encountered was 1 . Tolerances were taken to be ± 0.01 (i.e. 1% of the largest coefficient) for all coef-

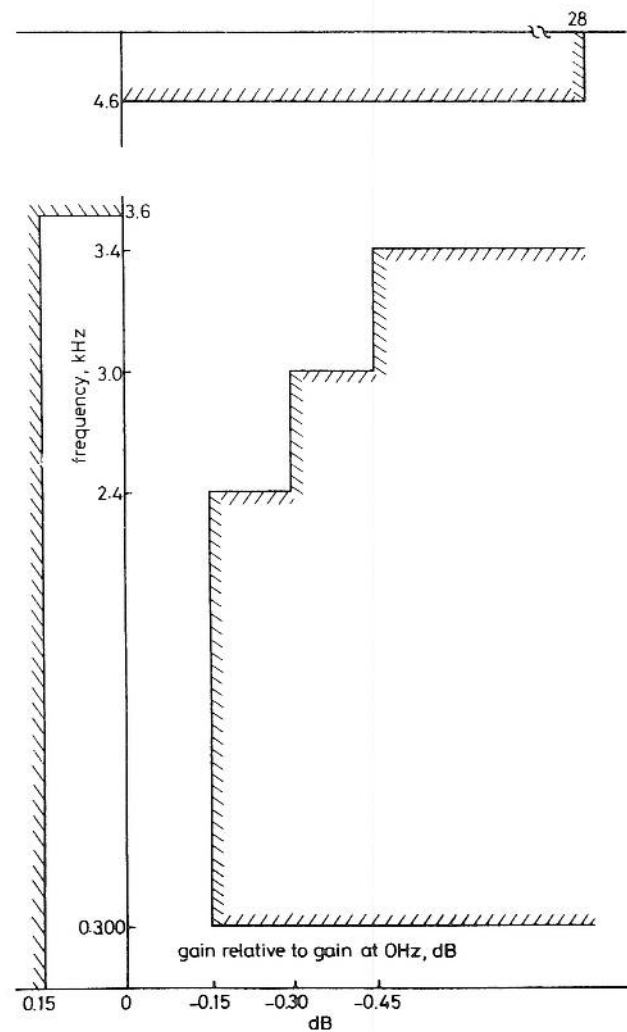


Fig. 11 Performance requirements for transversal filter

ficients. In the absence of accurate information about the statistical distributions of coefficient values, the choice of uniform distributions was considered prudent for a preliminary attempt at improving the design. The results obtained are shown in Fig. 12. Substantial increases in yield were obtained and the results lend support to the assertion that Monte Carlo based methods are relatively independent of dimensionality.

6.3 Active filter circuit

Several methods of design centering^{1,2,9} require the region of acceptability to be both connected and convex. Recently, Styblinski *et al.*⁸ have shown that, for a circuit in common use and subject to particular performance constraints, the region of acceptability is not simply connected. The circuit in question is a Sallen-Key type band-

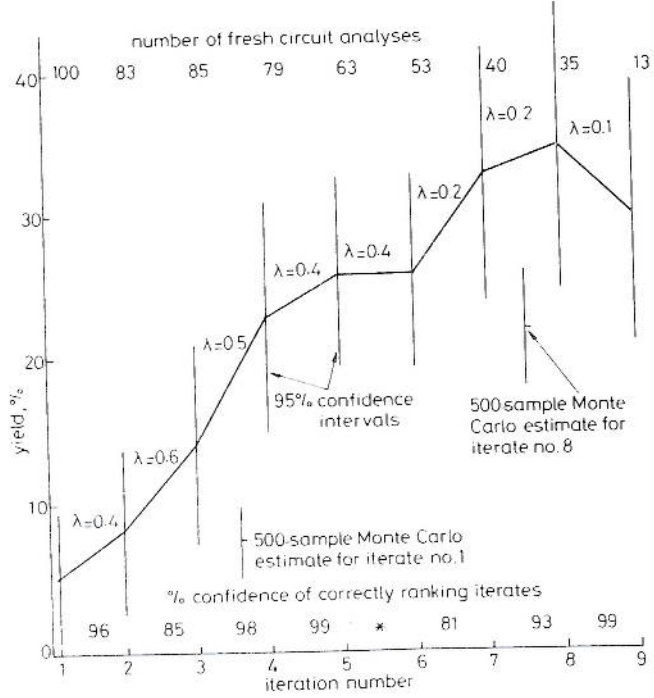


Fig. 12 Yield trajectory obtained by application of the centres-of-gravity design-centering algorithm to a 43-coefficient transversal filter

*No apparent increase in yield between iterations 5 and 6

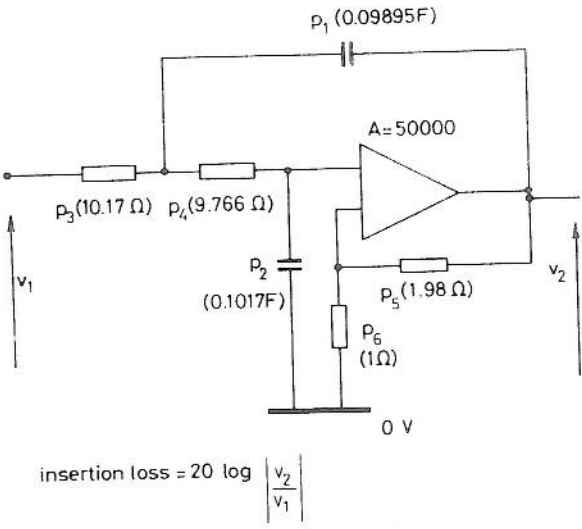


Fig. 13 Sallen-Key filter example

pass filter. The relevant circuit diagram and performance requirements are shown in Figs. 13 and 14.

For this example, the region of acceptability is not simply connected. In other words, it has a region of non-acceptability surrounded by a larger region of acceptability. To illustrate this condition, Fig. 15 depicts a section through the region of acceptability. The 2-dimensional section was computed by maintaining, at their nominal values, all the components except p_3 and p_4 , systematically varying the values of p_3 and p_4 and, for each such combination, analysing the circuit and testing against performance requirements.

Fig. 16 shows the result of applying the design-centering algorithm to this circuit, using a sample size of 100. The result indicated a modest yield increase from 58% to 69% in three iterations involving a total of 170 circuit analyses. Confirmatory 500-sample Monte Carlo analyses were carried out using the design centres of the first and fourth iterates, and showed an increase in yield from 57% to 65%. For the first and fourth iterations, and for components 3 and 4, a 2-dimensional section of the tolerance region is shown in Fig. 15.

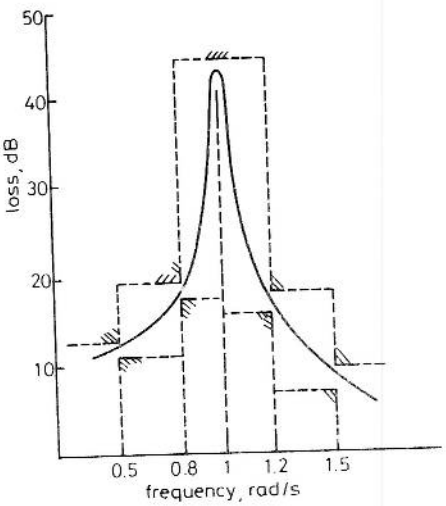


Fig. 14 Specifications and typical response for Sallen-Key filter example

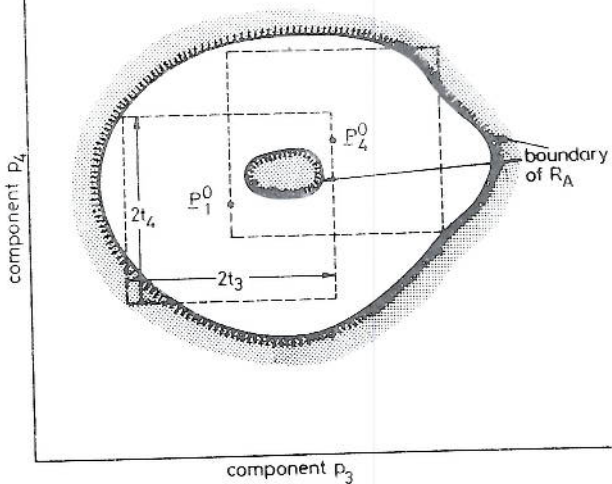


Fig. 15 Section, along axes associated with components 3 and 4, of the multiparameter component space associated with the Sallen-Key filter example, showing region of acceptability and location of tolerance regions corresponding to first and last iterations of design-centering procedure (see Fig. 16)

The above results lend support to the assertion that our statistical exploration approach to design centering is not limited to connected regions of acceptability.

7 Conclusions

The centres-of-gravity algorithm possesses desirable properties that make it a serious candidate for use in tolerance design. Its most attractive features are that it appears not to require an inordinate amount of computational effort to deal with circuits containing a large number of tolerated components, and that it is insensitive to nonconvexity and nonconnectivity of the region of acceptability. It is equally applicable to linear and nonlinear circuits and, since it requires only the evaluation of circuit responses and not their derivatives with respect to component values, can

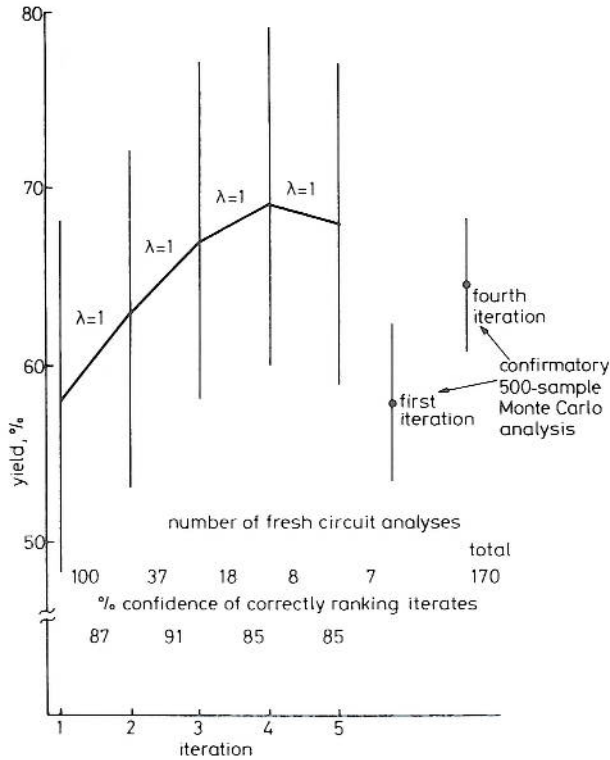


Fig. 16 Yield trajectory obtained by application of centres-of-gravity design centering algorithm to Sallen-Key filter example

(and has been) 'bolted on' to an existing circuit-analysis package.¹⁰ When compared with other statistically based methods of design centering, the centres-of-gravity algorithm performs favourably regarding the number of samples required in each of the Monte Carlo analyses.

Although extensively tested and suited to practical application, further improvements could usefully be made to the centres-of-gravity algorithm. Overall, it must be remarked that the algorithm, in common with many other direct-search optimisation schemes, has a strong heuristic basis, and that additional theoretical underpinning would be beneficial.

A number of specific opportunities for improvement and extension can be identified. For example, in view of its importance for integrated circuit design, the extension of the algorithm to correlated parameters should be explored. Also, an improved basis for the choice of step length λ (especially when the yield is low) would further assist the designer in his interaction with the optimisation. The influence on the design-centering process of the Monte Carlo sample size is clearly many-faceted and complex,

especially in those situations where the designer is afforded the opportunity of taking extra samples in order to increase the confidence of correct yield ranking. Therefore, further research into questions of sample size would be beneficial and particularly relevant in circumstances, such as the study of time-domain behaviour, where each circuit analysis is expensive.

8 Acknowledgments

The authors wish to acknowledge helpful discussions with Edgar Laksberg, Kirpal Tahim and Robert Tung. Financial support from Standard Telephones and Cables, Ltd. and the UK Science Research Council is gratefully acknowledged.

9 References

- 1 DIRECTOR, S.W., and HACHTEL, G.D.: 'The simplicial approximation approach to design centering', *IEEE Trans.*, 1977, CAS-24, pp. 363-372
- 2 DIRECTOR, S.W., and HACHTEL, G.D.: 'A point basis for design centering'. IEEE Proceedings CAD Conference on electronic and microwave circuits', University of Hull, Hull, England, July 1977, pp. 41-46
- 3 BRAYTON, R.K.: 'Optimisation in CAD'. In 'Modern network theory - an introduction' (St. Saphorin, Georgi, 1978) p. 26
- 4 SOIN, R.S., and SPENCE, R.: 'Statistical design centering for electrical circuits', *Electron. Lett.*, 1978, 24, pp. 772-774
- 5 BECKER, P.W.: 'Finding the better of two designs by Monte Carlo techniques', *IEEE Trans.*, 1974, R-23, pp. 242-246
- 6 PINEL, J.F., and ROBERTS, K.A.: 'Tolerance assignment in linear networks using nonlinear programming', *ibid.*, 1972, CT-19, pp. 475-479.
- 7 KNAUER, K., PFLEIDERER, H.J., and KELER, H.: 'CCD transversal filters with parallel-in/serial-out configuration', *Siemens Forsch. & Entwicklungsber.*, 1978, 7, p.3
- 8 STYBLINSKI, M., OGRODSKI, J., and OPALSKI, M.: 'Acceptability regions of a class of linear networks'. IEEE, Proceedings ISCAS 1980, pp. 187-191
- 9 BANDLER, J.W.: 'Optimisation of design tolerances using nonlinear programming', *J. Optimiz. Theory & Appl.*, 1974, 14, pp. 99-114
- 10 BURGESS, J.P., and SPENCE, R.: 'BASECAP user's manual' (Department of Electrical Engineering, University of New Brunswick, Canada, 1980)

10 Appendixes

10.1 Definition of yield

As before, $P = p_1, p_2, \dots, p_K$ is a set of parameter values defining a circuit. Let $\phi(P, P^0, T)$ be the K -dimensional joint probability density function describing the statistical distribution of the component parameter values. We define $g(P)$ as a testing function, such that

$$g(P) = 1 \quad \text{if } \underline{f}_i \leq f_i(P) \leq \bar{f}_i \\ = 0 \quad \text{otherwise}$$

where f_i, \underline{f}_i and \bar{f}_i are defined in the main text.

Then \bar{y} is the expectation of $g(P)$ with respect to $\phi(P, P^0, T)$:

$$Y = \langle g(P) \rangle = \int_{p_K^0 - t_K}^{p_K^0 + t_K} \dots \int_{p_1^0 - t_1}^{p_1^0 + t_1} g(P) \phi(P, P^0, T) \\ \times dp_1, dp_2, \dots, dp_K$$

10.2 An algorithm for statistical design centering using the correlated sampling scheme

Step 1:

Set counter $M = 1$. Set speed of pseudorandom generator to some known value denoted by RL .

Step 2:

Perform Monte Carlo analysis with design centre P_M^o ; p.d.f $\phi(P, P_M^o, T)$, sample size N_M . Estimate yield Y_M . If $M = 1$, go to step 4.

Step 3:

Estimate ΔY_{M-1} , where

$$\Delta \hat{Y}_{M-1} = \hat{Y}_M - \hat{Y}_{M-1}$$

Estimate confidence of correct ranking, i.e. confidence of being correct about the sign of ΔY_{M-1} . If confidence is not high enough, go to step 6. If confidence is sufficient and $\Delta \hat{Y}_{M-1}$ is negative, STOP.

Step 4:

Examine parameter values of sample circuits of the M th Monte Carlo analysis. Determine new design centre

$$P_{M+1}^o = P_M^o + \lambda_M(G_{P_M} - G_{F_M})$$

Step 5:

Reset random seed to value RL . Increment counter, $M = M + 1$. Go to step 2.

Step 6:

Generate and analyse more random circuits in addition to the number already analysed. Go to step 3.

10.3 Algorithm for statistical design centering using the common points scheme

Step 1:

Set counter $M = 1$. Select N , the 'available sample size'. Let $N_1 = N$.

Step 2:

Perform Monte Carlo analysis. Sample size N_1 , design centre P_1^o .

Step 3:

Determine the new design centre

$$P_{M+1}^o = P_M^o + \lambda_M(G_{P_M} - G_{F_M})$$

on the basis of the N available samples.

Step 4:

Determine regions A, B, C (see Fig. 4). From the N circuit samples identify and determine the numbers N_A and $(N - N_A)$ respectively falling in regions A and B . Estimate partial yields Y_A and Y_B . Discard samples in region A . This leaves $(N - N_A)$ samples available for reuse.

Step 5:

Perform modified Monte Carlo analysis. Generate and analyse N_A random (with a uniform distribution) circuits distributed in region C . Therefore a total of N samples will now be available for determining the new design centre (see step 6).

Step 6:

Estimate partial yield Y_C and hence estimate yield \hat{Y}_{M+1} as $Y_{M+1} = \hat{Y}_B V_B + \hat{Y}_C V_C$. Estimate the difference in partial yield $\Delta P\hat{Y} = \hat{Y}_C - \hat{Y}_A$. Compute the confidence of correctly ranking the M th and $(M + 1)$ th iterates. If confidence of correct ranking is insufficient, go to step 8. If confidence of correct ranking is sufficient and $\Delta \hat{Y}_M$ is negative, STOP.

Step 7:

Increment counter. $M = M + 1$. Go to step 3.

Step 8:

Perform more circuit analyses in regions A and C . Go to step 6.



Dr. Robert Spence is a Reader in Electrical Engineering at Imperial College, London. His research interests lie mainly in the field of computer-aided circuit design and its associated man-computer interaction, and the field of tolerance analysis and design. He was the principal architect of the MINNIE interactive-graphic system for circuit design and, with his colleagues, was responsible for a number of

algorithms for the efficient sensitivity analysis of circuits. Recently, he has been involved in devising a new approach to the teaching of computer-aided circuit design. Dr. Spence is the author of 'Linear active networks' (1970) and 'Resistive circuit theory' (1974) and co-author of 'Tellegen's theorem and electrical networks' (1970), 'Modern network theory - an introduction' (1978) and 'Computer-aided electronic circuit design: sensitivity and optimization' (1980). He is co-editor of the *IEE Journal on Electronic Circuits and Systems (IEE Proceedings Part G)*, and was an Associate Editor of the *IEEE Transactions on Circuits and Systems*. He also acts as general editor of a series of volumes on the computer-aided design of electronic circuits being published by Scientific Elsevier of Amsterdam. Dr. Spence is a Fellow of the IEE, and in 1977 was awarded the Fellowship of the Institute of Electrical and Electronic Engineers (IEEE) for 'contributions to the theory of, and education in, the algorithmic, linguistic and perceptual aspects of computer-aided circuit design'.



Dr. Randeep Singh Soin received the B.Sc.(Eng.) A.C.G.I. degree from the Imperial College of Science and Technology, University of London, in 1974. From 1974 to 1975 he was employed by Pye TMC Ltd. in Kent where he was engaged in development of p.c.m. line systems, during which he was seconded to Philips Telecommunicatie Industrie in the Netherlands, where he worked on fault location systems for digital regenerators. He returned to Imperial College in 1975 as a research student and in 1980 received the Ph.D. degree for his work on algorithms for tolerance design. Since September 1979 he has been with Philips Research Laboratories, where he continues his work on tolerance analysis and design.